

## Four Element MIMO DRA with High Isolation for WLAN Applications

Goffar A. Sarkar<sup>1, \*</sup>, Suparna Ballav<sup>1</sup>, Ayan Chatterje<sup>2</sup>,  
Subarna Ranjit<sup>1</sup>, and Susanta K. Parui<sup>1</sup>

**Abstract**—A dielectric resonator (DR) based MIMO (Multiple Input Multiple Output) antenna with enhanced isolation is proposed in this letter. The proposed MIMO antenna consists of four hemispherical shaped dielectric resonator (HDR) radiating at 4.9 GHz. The isolation between two consecutive radiators is enhanced by rotating feeding line of one element at an angle of 180°. The antenna is studied in terms of *S*-parameters, gain, envelope correlation coefficient (ECC), channel capacity loss (CCL), and diversity gain (DG). All the parameters are found to be within acceptable range. The proposed design is fabricated, and it is found that measured results are in good agreement with simulation.

### 1. INTRODUCTION

The recent evolution in wireless communications requires systems with high reliability and capacity. Due to limited channel capacity and data rate of single input single output (SISO) system, it becomes difficult for a SISO system to meet the requirements of today's wireless communication system. For these requirements multi input multi output (MIMO) came into existence. In MIMO technology, multiple antennas are used in both the transmitter and receiver ends to improve reliability, stability, and capacity without any increment of channel bandwidth [1]. However, multiple antennas increase the size of the devices. Space being one of the main constraints of today's compact wireless communication systems, it is highly desirable to etch out multiple radiators in a single substrate with high degree of isolation [2]. In last few decades, researchers mainly focused on patch based MIMO antenna as it is easy to integrate with portable wireless devices. However, patch based MIMO antennas have limitations in high frequency application for their metallic losses. In that scenario, dielectric resonator antennas (DRAs) come into existence for MIMO application. DRAs have lots of attractive features such as high efficiency, wide bandwidth, and high gain [3].

As said, MIMO antenna elements should be etched on the same substrate with high isolation between ports for designing compact wireless systems. Several isolation techniques have been demonstrated in the literature for planar antennas. In order to achieve the best performance of MIMO antenna systems, isolation is accomplished by orthogonal feeding techniques [4] and [5]. Defected ground structures (DGSs) are used to suppress surface wave, which leads to improvements of isolation in [6–8]. In [9, 10], various decoupling networks are used which introduce negative coupling between adjacent ports and cancel the cause of coupling between them. Ketzaki and Yioultsis placed split ring resonators (SSRs) in between two monopoles to reduce the coupling between antenna elements [11]. Zhang and Pedersen [12] and Yang et al. [13] used neutralization line (NL) to achieve high isolation in MIMO systems. However, very few reports are published on mutual coupling reduction on DRA based MIMO antenna. A dual polarized MIMO DRA is presented in [14], and good isolation is achieved by exciting orthogonal mode with the cost of complex feeding networks. In [15], a MIMO DRA for LTE applications

---

*Received 13 March 2019, Accepted 22 May 2019, Scheduled 31 May 2019*

\* Corresponding author: Goffar Ali Sarkar (goffar.ali@gmail.com).

<sup>1</sup> Department of Electronics and Telecommunication Engineering, Indian Institute of Engineering Science and Technology, Shibpur, India. <sup>2</sup> Department of Electronics and Communication Engineering, Nation Institute of Technology Sikkim, India.

is presented, and ground plane is modified for isolation improvement. It should be noted that insertion of rectangular DRA within the substrate increases fabrication complexity. Metallic strips and inverted L-shaped strips have been utilized in [16] for isolation improvements. A compact MIMO antenna is presented in [17] using CPW conformal stripline and microstripline fed conformal stripline. Wrapping of metallic strips on DRAs makes the fabrication difficult. A two-element MIMO antenna with L-shaped and rectangular shaped DGSs on ground plane was studied and achieved 18 dB isolation by Kumari et al. [18].

In this paper, a four-element DRA based MIMO antenna with high isolation is proposed at 4.9 GHz for WLAN applications which is mainly dedicated for public safety entities. The isolation between two consecutive elements of the MIMO antenna excited from same side is observed as  $-15$  dB. In order to improve the isolation between the elements, they are fed from opposite side. Therefore, magnetic fields excited inside the radiators are  $180^\circ$  (out of phase) with respect to each other which effectively reduce the magnetic coupling and improve the isolation by 5 dB. For further enhancement of the isolation, both the radiators are placed in an offset position that improves the isolation by another 6 dB leading to an overall isolation enhancement of around 11 dB without degrading the radiation performance. Moreover, ECC, DG, and CCL are studied, and results show that a WLAN MIMO antenna with high isolation is achieved.

## 2. ANTENNA DESIGN

### 2.1. Modes and Resonance Frequency

Transverse electric (TE) mode and transverse magnetic (TM) mode are supported by hemispherical DRA. For TE mode,  $E_r$  and  $E_\phi$  vanish at  $\theta = 90^\circ$ , whereas for TM mode field vanishes at  $\theta = 0^\circ$ . The lowest order TE mode is  $TE_{111}$ , and that for TM is  $TM_{101}$ . From field continuity for  $TE_{111}$  mode at the surface of a hemisphere of radius  $R$ , a transcendental equation is obtained as [19]:

$$\frac{\hat{J}_1(kR)}{\hat{J}'_1(kR)} = \varepsilon_r^{1/2} \frac{\hat{H}_1(k_0R)}{\hat{H}'_1(k_0R)} \quad (1)$$

where  $\hat{J}_1(x) = xj_1(x)$ ,  $\hat{H}_1(x) = xh_1^{(2)}(x)$ ,  $j_1(x)$  is the spherical Bessel function of first order,  $h_1^{(2)}(x)$  the spherical Hankel function of the first order second kind,  $k =$  wave number in dielectric,  $k_0 =$  wave number in free space,  $k = \varepsilon_r^{1/2}k_0$ . Equation (1) is numerically solved for complex quantity  $kR = \text{Re}(kR) + j\text{Im}(kR)$ , and resonant frequency is found as:

$$f_r = \frac{4.775 \times 10^7 \text{Re}(kR)}{\sqrt{\varepsilon_r}R} \quad (2)$$

The dimension of the HDRA is calculated from Eq. (2).

### 2.2. Single Element Configuration

The antenna is designed on a substrate having dielectric constant 2.7, loss tangent 0.0023, and height ( $H$ ) 0.79 mm as shown in Fig. 1. The antenna consists of a hemisphere-shaped dielectric resonator (DR) with radius ( $r$ ) of 7.5 mm. The relative permittivity and loss tangent of this DR are 20 and 0.002, respectively. The antenna is fed by a  $50 \Omega$  microstrip line and simulated using HFSS. The antenna provides the resonance at 4.9 GHz with 5.1% impedance bandwidth as shown in Fig. 1(b). A parametric study is done by varying the inserted length ( $L_{S0}$ ) of the microstrip line underneath the DR element in order to achieve optimized reflection coefficient as evident in Fig. 1(c). All dimensions of the single element antenna are given in Fig. 1.

### 2.3. MIMO Antenna Configuration

The MIMO antenna is configured using the antenna designed in Section 2.2. Fig. 2(a) depicts the geometry of the proposed MIMO antenna. The gap between two antenna elements is major constraints in MIMO configuration. In this design, a gap ( $d_0$ ) of 15 mm is considered between two consecutive

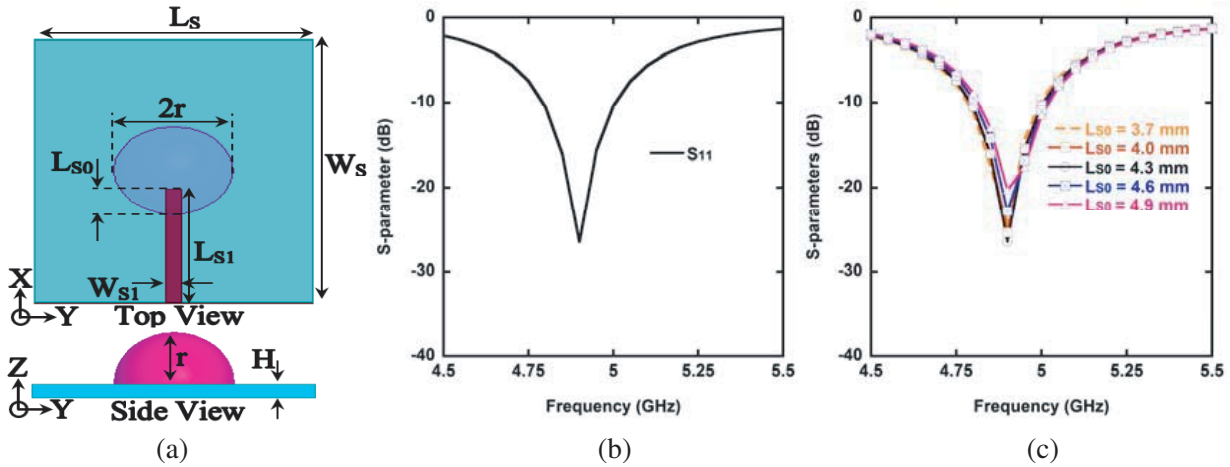


**Figure 1.** (a) Single element HDRA ( $L_S = 35$ ,  $L_{S0} = 4.3$ ,  $L_{S1} = 19.3$ ,  $W_S = 45$ ,  $W_{S1} = 2.1$  (all dimensions are in mm)), (b)  $|S_{11}|$  at  $L_{S0} = 4.3$  mm and (c)  $|S_{11}|$  for different values of  $L_{S0}$ .

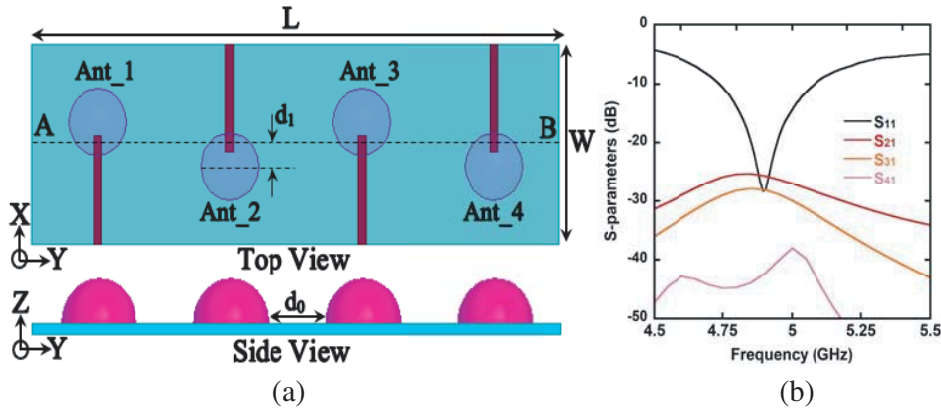


**Figure 2.** (a) Proposed geometry and (b) simulated  $S$ -parameters.

radiators, and they are placed in an offset position ( $d_1$ ) of 5 mm from centre line (AB) of the substrate to achieve more than 25 dB isolation. The substrate area of this proposed MIMO antenna is 140 mm  $\times$  45 mm. As the antenna elements are placed in symmetric fashion, only four  $S$ -parameters out of sixteen are shown in Fig. 2(b). The MIMO antenna provides  $|S_{11}|$  as single element antenna, and  $|S_{21}|$  is observed better than 25 dB.

**2.4. Isolation Improvement**

The design steps of isolation improvement between two consecutive antenna elements are elaborated in this section and picturized in Figs. 3(a)–3(c). At first, two antenna elements are placed side by side with a separation of 15 mm as Antenna\_A and achieve 15 dB isolation as shown in Fig. 4(a). After that, feeding line of one element is rotated by 180° in azimuthal plane ( $XY$  plane) and achieves 20 dB of isolation as shown in Fig. 4(a). To get physical insight of isolation enhancement in Antenna\_B, we have studied the magnetic fields inside the two DRAs, shown in Fig. 4(b). It is observed that the magnetic fields orientations inside these two DRAs are 180° (out of phase) to each other. These opposite magnetic vector fields result in low coupling between these two antenna elements. The positions of DRAs are further modified such that Ant\_1 is shifted towards positive  $X$ -axis whereas Ant\_2 is shifted towards negative  $X$ -axis, which makes an offset of 10 mm between the centres of two DRAs as shown in Fig. 3(c) (Antenna\_C). In this design, 6 dB more isolation is achieved with respect to Antenna\_B as evident in Fig. 4(a).

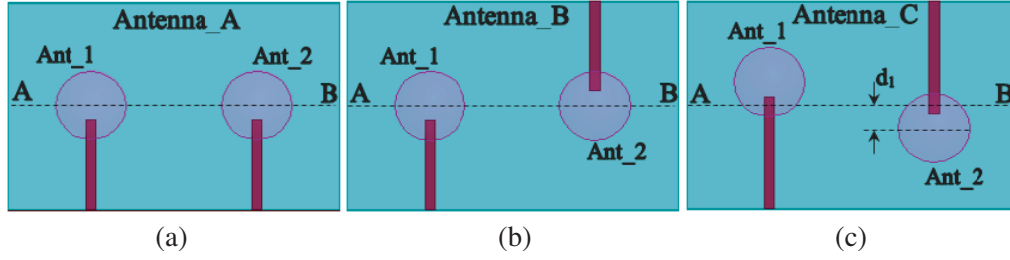


**Figure 3.** Two element MIMO configurations, (a) Antenna\_A, (b) Antenna\_B and (c) Antenna\_C.

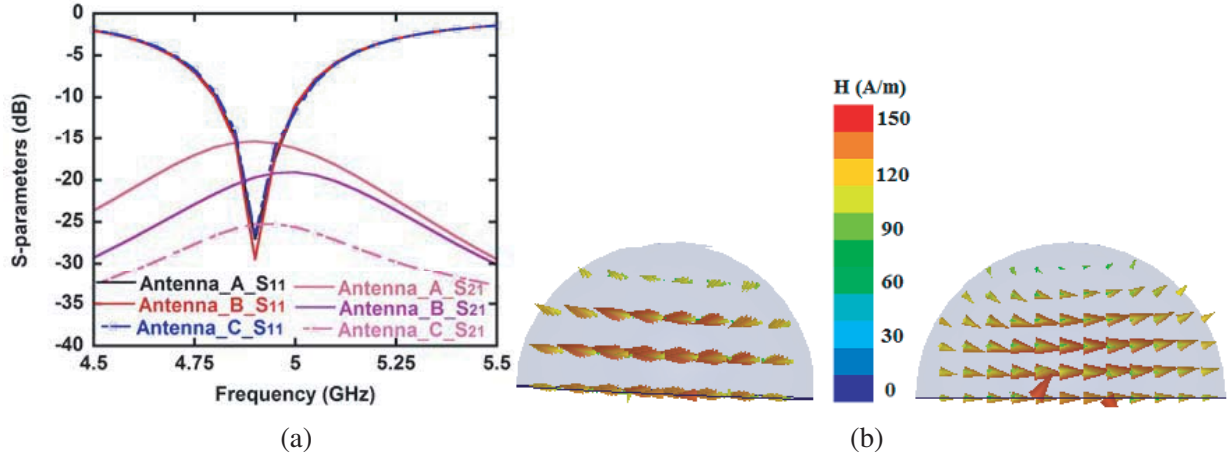


**Figure 4.** (a)  $S$ -parameters of different MIMO configurations and (b) magnetic field distribution inside the two DRAs of Antenna\_C (from left Ant\_1 and Ant\_2).

### 3. EXPERIMENTAL RESULTS

An Arlon AD270 (relative permittivity 2.7 and loss tangent 0.0023) substrate is used to fabricate the proposed MIMO antenna, shown in Fig. 5(a).  $S$ -parameters are measured using a Vector Network Analyzer by Anritsu (MS2025B), and simulated and measured results are plotted in Figs. 5(b)–5(c). A little bit discrepancy is observed in measured results due to manual fabrication. Radiation patterns along  $E$ -plane ( $XZ$ -plane) and  $H$ -plane ( $YZ$ -plane) are measured by exciting Ant\_1 when all other antennas are matched with  $50\ \Omega$  matched ports. Simulated and measured radiation patterns of  $E$ -plane and  $H$ -plane are plotted in Figs. 6(a) and 6(b), respectively. The co-polar radiation pattern is observed maximum in broadside direction. The cross-polar performance is well acceptable as it is below 30 dB with respect to co-pol. The gain of this antenna is obtained as 6.2 dBi at the resonant frequency.

The performances of MIMO antenna cannot be assessed by isolation only. There are several parameters such as envelope correlation coefficient (ECC), diversity gain (DG), and channel capacity loss (CCL) have to be studied to evaluate performances of a MIMO antenna. ECC reveals the correlation between the signals transmitted and received by the antennas. It is accurate to compute ECC from far-field radiation patterns by Eq. (3) in [2].

$$\rho_e = \frac{\left| \iint_{4\pi} [\vec{F}_1(\theta, \phi) * \vec{F}_2(\theta, \phi)] d\Omega \right|^2}{\iint_{4\pi} |\vec{F}_1(\theta, \phi)|^2 d\Omega \iint_{4\pi} |\vec{F}_2(\theta, \phi)|^2 d\Omega} \quad (3)$$

where  $\vec{F}_i(\theta, \phi)$  is the 3D far-field pattern of the radiator when excitation is given to the  $i$ th port,  $\Omega$  the

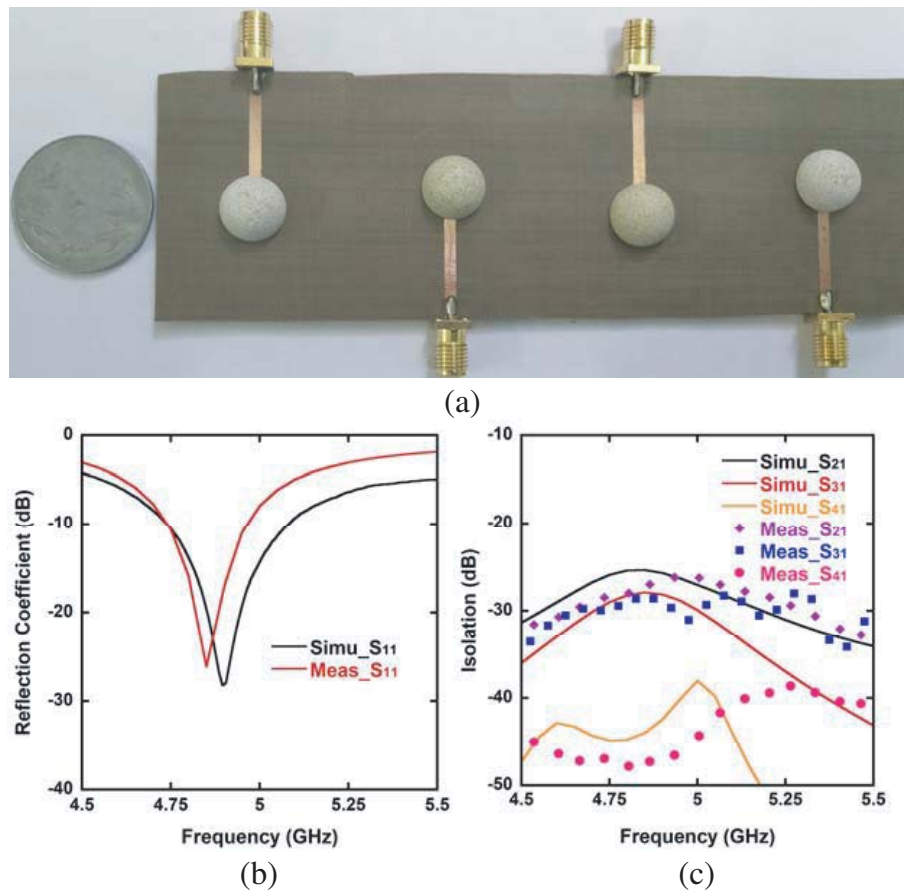


Figure 5. (a) Fabricated prototype, (b) simulated and measured  $|S_{11}|$  and (c) isolations.

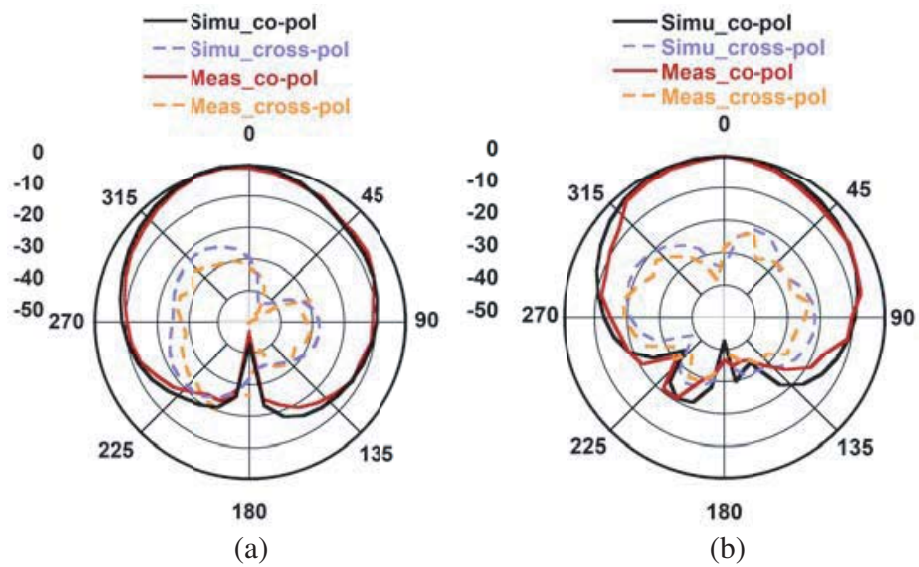
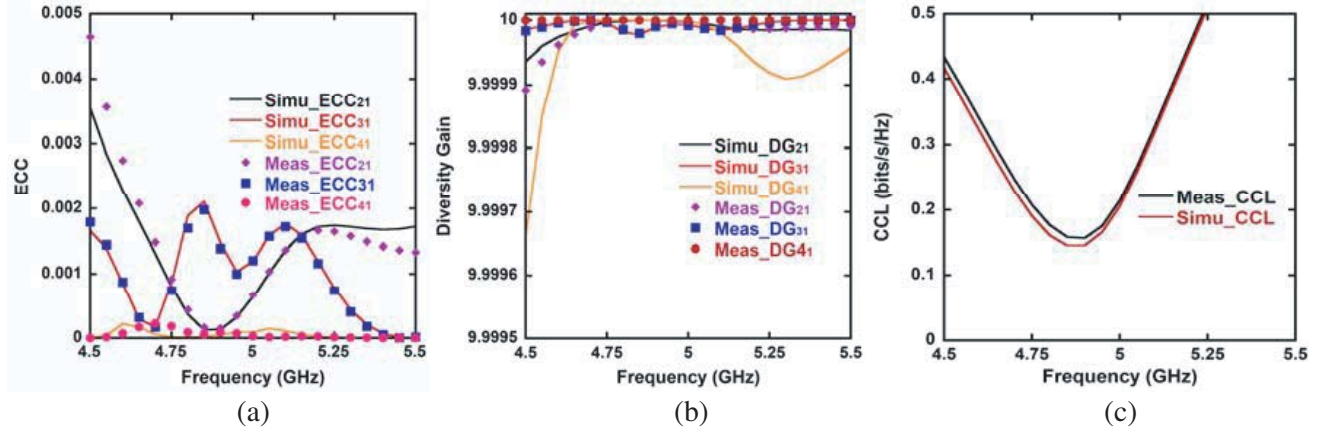


Figure 6. Simulated and measured radiation patterns in (a)  $E$ -plane and (b)  $H$ -plane.



**Figure 7.** Simulated and measured results of the proposed MIMO antenna, (a) ECC, (b) diversity gain (DG) and (c) CCL.

**Table 1.** Comparison of proposed MIMO DRA with previous works.

Ref. no.	Techniques	Fabrication Difficulties	Isolation (dB)	ECC	DG	CCL (bits/s/Hz)
[15]	Slits on ground plane	Complex	20	0.054	> 9.680	-
[16]	Dual strips along with reflector	Complex	15	0.2	-	-
[17]	Orthogonal mode and ground plane	Complex	18	0.25	-	-
[18]	L-shaped and rectangular shaped DGSs	Easy	18	0.21	> 9.110	0.4
<b>This work</b>	<b>Out of phase magnetic field</b>	<b>Easy</b>	<b>25</b>	<b>0.002</b>	<b>&gt; 9.999</b>	<b>0.2</b>

solid angle, and (\*) the Hermitian product operator. Also, in the case of highly efficient antenna system (> 90%), ECC can be calculated from  $S$ -parameters as given by Eq. (4) which is less laborious.

$$\rho_e = \frac{|S_{11}^* S_{12} + S_{21}^* S_{22}|^2}{(1 - |S_{11}|^2 - |S_{21}|^2)(1 - |S_{12}|^2 - |S_{22}|^2)} \quad (4)$$

where  $S_{ii}$  represents the reflection coefficients, and  $S_{ij}$  represents the isolation between the  $i$ th and  $j$ th ports. The simulated and measured ECCs of the proposed MIMO antenna are calculated using  $S$ -parameters and displayed in Fig. 7(a). From Fig. 7(a), it is observed that the ECC value is less than 0.002 over the operating band where the practical limit of ECC is 0.5. The obtained ECC value guarantees good diversity performance of this proposed design. The improvement of signal to noise ratio (SNR) in multiport antenna system with respect to single port antenna system is measured by diversity gain [2]. Diversity gain of this proposed antenna system is calculated by using the following equation [20]:

$$DG = 10\sqrt{1 - |\rho_e|^2} \quad (5)$$

where  $\rho_e$  is the ECC. The diversity gain calculated using Equation (5) is shown in Fig. 7(b). From Fig. 7(b), it is noticed that the simulated and measured values of DG are about 10 at operating band. The upper limit of message transmission or reception rate over a communication channel is defined by

channel capacity loss (CCL). Channel capacity using  $S$ -parameter can be calculated as [21]:

$$C_{\text{loss}} = -\log_2 \det(\Psi^R) \quad (6)$$

where

$$\Psi^R = \begin{bmatrix} \Psi_{11} & \Psi_{12} \\ \Psi_{21} & \Psi_{22} \end{bmatrix}$$

$$\Psi_{11} = 1 - \left( |S_{11}|^2 + |S_{12}|^2 \right)$$

$$\Psi_{22} = 1 - \left( |S_{21}|^2 + |S_{22}|^2 \right)$$

$$\Psi_{12} = -(S_{11}^* S_{12} + S_{21}^* S_{22})$$

$$\Psi_{21} = -(S_{22}^* S_{21} + S_{12}^* S_{11})$$

The calculated CCLs from simulated and measured  $S$ -parameters are shown in Fig. 7(c), and it is found that CCL value is within acceptable limit (less than 0.2 bits/s/Hz) at operating band.

Table 1 highlights that the proposed technique is simpler and provides better performances than in published literature [15–17]. The design in [18] is easy in terms of fabrication; however, the proposed design provides better isolation. It is also noted that in terms of diversity performance (ECC, DG, CCL), the proposed design is the best candidate.

#### 4. CONCLUSION

A four-element MIMO antenna with improved isolation is proposed for WLAN applications. The antenna elements are excited in such a way that the magnetic fields are canceled between each other to improve isolation.  $S$ -parameters are studied, and it is found that more than 25 dB isolation is achieved between antenna elements. Radiation patterns validate the broadside radiation with peak gain of 6.2 dBi, and cross-polar performance is quite good. ECC, DG, and CCL are studied to comment on the diversity performance of the proposed antenna, and it is observed that all the parameters are within acceptable limit.

#### REFERENCES

1. Costa, J. R., E. B. Lima, C. R. Medeiros, and C. A. Fernandes, "Evaluation of a new wideband slot array for MIMO performance enhancement in indoor WLANs," *IEEE Trans. Antennas Propag.*, Vol. 59, No. 4, 1200–1206, 2011.
2. Sharawi, M. S., *Printed MIMO Antenna Engineering*, Artech House, USA, 2014.
3. Petosa, A., *Dielectric Resonator Antenna Handbook*, Artech House, USA, 2007.
4. Zhang, Y. and B. Niu, "Compact Ultrawideband (UWB) slot antenna with wideband and high isolation for MIMO applications," *Progress In Electromagnetics Research C*, Vol. 54, 9–16, 2014.
5. Liu, L., S. W. Cheung, and T. Yuk, "Compact MIMO antenna for portable UWB applications with band-notched characteristic," *IEEE Trans. Antennas Propag.*, Vol. 63, No. 5, 1917–1924, 2015.
6. Mao, C.-X., Q.-X. Chu, Y.-T. Wu, and Y.-H. Qian, "Design and investigation of closely-packed diversity UWB slot-antenna with high isolation," *Progress In Electromagnetics Research C*, Vol. 41, 13–25, 2013.
7. Liu, L., S. W. Cheung, and T. I. Yuk, "Compact MIMO antenna for portable devices in UWB applications," *IEEE Trans. Antennas Propag.*, Vol. 61, No. 8, 4257–4264, 2013.
8. Luo, C. M., J. S. Hong, and L. L. Zhong, "Isolation enhancement of a very compact UWB-MIMO slot antenna with two defected ground structures," *IEEE Antennas Wireless Propag. Lett.*, Vol. 14, 1766–1769, 2015.
9. Yu, Y., Y. Jiang, W. Feng, S. Mbayo, and S. Chen, "Compact multiport array with reduced mutual coupling," *Progress In Electromagnetics Research Letters*, Vol. 39, 161–168, 2013.

10. Khan, M. S., A. D. Capobianco, A. I. Najam, I. Shoaib, E. Autizi, and M. F. Shafique, "Compact ultra-wideband diversity antenna with a floating parasitic digitated decoupling structure," *IET Micr. Antennas Propag.*, Vol. 8, No. 10, 747–753, 2014.
11. Ketzaki, D. A. and T. V. Yioultis, "Metamaterial-based design of planar compact MIMO monopoles," *IEEE Trans. Antennas Propag.*, Vol. 61, No. 5, 2758–2766, 2013.
12. Zhang, S. and G. F. Pedersen, "Mutual coupling reduction for UWB MIMO antennas with a wideband neutralization line," *IEEE Antennas Wireless Propag. Lett.*, Vol. 15, 166–169, 2015.
13. Yang, Y., Q. Chu, and C. Mao, "Multiband MIMO antenna for GSM, DCS, and LTE indoor applications," *IEEE Antennas Wireless Propag. Lett.*, Vol. 15, 1573–1576, 2016.
14. Zou, L., D. Abbott, and C. Fumeaux, "Omnidirectional cylindrical dielectric resonator antenna with dual polarization," *IEEE Antennas Wireless Propag. Lett.*, Vol. 11, 515–518, 2012.
15. Nasir, J., M. H. Jamaluddin, M. Khalily, M. R. Kamarudin, and I. Ullah, "Design of an MIMO dielectric resonator antenna for 4G applications," *Wireless Person. Comm.*, Vol. 88, No. 3, 525–536, 2016.
16. Sharma, A., G. Das, and R. K. Gangwar, "Dual polarized triple band hybrid MIMO cylindrical dielectric resonator antenna for LTE2500/WLAN/WiMAX applications," *Int. J. RF Microw. Comp. Eng.*, Vol. 26, No. 9, 763–772, 2016.
17. Das, G., A. Sharma, R. K. Gangwar, and M. Sharawi, "Compact back to back DRA based four port MIMO antenna system with bi-directional diversity," *Electronics Lett.*, Vol. 54, No. 14, 884–886, 2018.
18. Kumari, T., G. Das, A. Sharma, and R. K. Gangwar, "Design approach for dual element hybrid MIMO antenna arrangement for wideband applications," *Int. J. RF Microw. Comp. Eng.*, 2018, 10.1002/mmce.21486.
19. Mcallister, M. W. and S. A. Long, "Resonant hemispherical dielectric antenna," *Electronics Lett.*, Vol. 20, No. 16, 657–659, 1984.
20. Nasir, J., M. H. Jamaluddin, M. Khalily, M. R. Kamarudin, I. Ullah, and R. Selvaraju, "A reduced size dual port MIMO DRA with high isolation for 4G applications," *Int. J. RF Microw. Comp. Eng.*, Vol. 25, No. 6, 495–501, 2015.
21. Islam, S. N., M. Kumar, G. Sen, and S. Das, "Design of a compact triple band antenna with independent frequency tuning for MIMO applications," *Int. J. RF Microw. Comp. Eng.*, 2018, 2018.10.1002/mmce.21620.